

# Switching Cells and Their Implications for Power Electronic Circuits

Leon M. Tolbert<sup>1</sup>, Fang Zheng Peng<sup>2</sup>, Faisal H. Khan<sup>3</sup> and Shengnan Li<sup>1</sup>

<sup>1</sup>The University of Tennessee, Department of Electrical Engineering and Computer Science, Knoxville, 37996-2100, USA

<sup>2</sup>Michigan State University, Department of Electrical and Computer Engineering, East Lansing, 48824, USA

<sup>3</sup>Electric Power Research Institute (EPRI), Knoxville, 37932, USA

**Abstract**-This paper will introduce two basic switching cells, P-cell and N-cell, along with their implications and applications in power electronic circuits. The concept of switching cells in power electronic circuits started in the late 1970's. The basic cells presented in this paper have one switching element (transistor) and one diode. The P-cell is the mirror circuit of the N-cell and vice-versa, and this paper suggests that (1) most power electronic circuits can be analyzed and re-constructed using these basic switching cells, (2) single, dual, and 6-pack switching modules should be configured and laid-out according to the basic switching cells and not necessarily the conventional way used by industry, and (3) many benefits such as minimal parasitic inductance and dead-time elimination or minimization may come about. The present paper will describe the construction and operation of these basic switching cells, and it will also show a sequential method to reconstruct several classical dc-dc converters, a voltage source inverter (VSI), and a current source inverter (CSI) using these basic switching cells. In addition, the use of basic switching cells introduces some new topologies of dc-dc converters that originate from the buck, boost, and Ćuk converter for negative input voltages. This paper will also illustrate the experimental results of the new and existing topologies constructed from basic switching cells.

## I. INTRODUCTION

As the basic elements, switching devices (mainly MOSFET and IGBT) and diodes along with inductors and capacitors are used in power electronic circuits to perform dc-dc, dc-ac, and ac-ac power conversion. In a piece-wise fashion, many circuits have been invented, proposed, and demonstrated to perform these power conversion uses [7]. The classical dc-dc converters like buck, boost, buck-boost, and Ćuk converters are used in various applications, and the modeling of these various structures are very important to design the control circuits for these converters [1-8]. However, these circuits have rarely been examined and investigated in terms of their relationships, topological characteristics, or what are their basic building blocks. To examine the basic building blocks of these dc-dc converters and dc-ac inverters, the authors proposed two basic switching cells [9].

These basic switching cells function as the fundamental

elements in power electronic circuits, which cannot be further broken down or apart and should be used as the basis for manufacturing/layout of single, dual, and 6-pack modules that semiconductor manufacturers are producing. Existing well-known circuits can easily be represented and configured from the basic switching cells. Moreover, some new conversion circuits can be derived. In the present paper, Section II will review switching cell's history; section III will describe the basic switching cell operation; section IV will illustrate the applications of these switching cells to introduce new kinds of power converters. Sections V and VI will present the experimental results as well as the discussion on the test results of several dc-dc converters. Finally, sections VII-VIII will discuss the use of basic switching cells in inverter applications.

## II. EXISTING SWITCHING CELLS

The introduction of the switching cell concept started with the canonical cell [10, 12] where an inductor, a capacitor, and a single-pole double throw switch form a basic canonical switching cell shown in Fig. 1. The cell has three terminals A, B, and C and each of them can be used as an input/output/common terminal. If terminal A is used as an input, B as an output and C is used as the common terminal; the canonical circuit forms one type of dc-dc converter. Six different combinations can be formed by changing the function of the three terminals in different combinations [7]. Among these six combinations, only three distinct effective circuits are found whereas the others are functionally the same. Thus, using these three combinations, the buck, boost, and buck-boost converter can be formed.

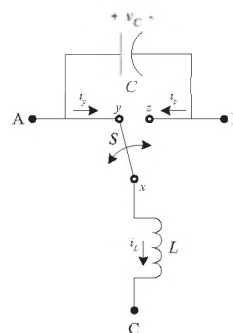


Fig. 1. Basic canonical cell.

Besides the canonical switching cell, there are many reported methods of modeling power electronic converters out of some switching modules or blocks. According to [12], the classical converters can be grouped into two major converter families - buck converter and boost converter. The buck family converters' small signal models can be expressed in terms of h-parameters, and those for the boost families are defined by g-parameters. When a unity feedback is applied in the buck converter, the buck-boost converter is formed.

Using the technique presented in [13], the classical PWM converters can be represented by only the buck and boost converter connected in cascaded arrangement, and the two-port network theory is applied. This method is reported as the graft scheme. The graft scheme presents a unified and systematic method to synthesize and model transformer-less PWM dc-dc converters. To do that, 4 different basic unit cells were presented where the cells are made from two transistors. Then using the graft scheme, the diode-transistor realizations for each of those 4 cells were derived.

### III. TWO BASIC SWITCHING CELLS

Fig. 2 shows the two basic switching cells defined in this paper. Each cell consists of one switching device (a MOSFET or IGBT) and one diode connected to three terminals: (+), (-), and (→) /or (←). Each cell has a common terminal which is shown as (→) /or (←) on the schematic. For the P-cell, this common terminal is connected to the positive terminal of a current source or an inductor. For an N-cell, this common terminal is connected to the negative of a current-source or an inductor. The active switching device in a P-cell is connected between the (+) and common terminal, whereas in an N-cell, the switching device is connected between the (-) terminal and the common terminal. Thus, the P-cell is the mirror circuit of the N-cell and vice versa [9].

The basic switching cells proposed in this paper are the practical implementation of the canonical switching cell found in [7]. Although the switching cells presented in this paper have only two components, they can be connected in different combinations to create various power electronic circuits.

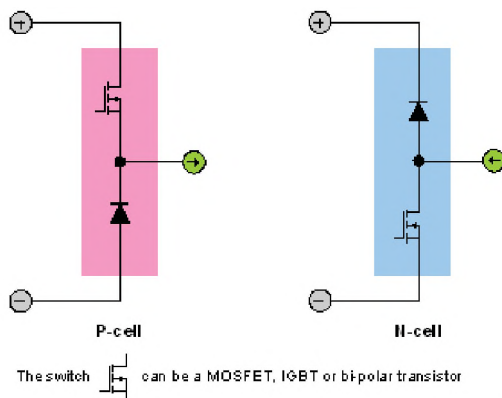


Fig. 2. Two basic switching cells: P-cell and N-cell.

### IV. DC-DC CONVERTERS FROM BASIC SWITCHING CELLS

Fig. 3 summarizes the four classical converters and their cell structures. In Fig. 3, there are three columns and each column has 4 figures. The figures in the leftmost column show the four major classical converters. These converters are made from inductors, capacitors, diodes and controlled switches. As stated previously, each of these converters can be expressed using the basic switching cells and the corresponding circuits are summarized in the middle column. The converters in this column are made from either N-cell or P-cell. Thus it is seen that except for the boost converter, all of the conventional converters have an inherent P-cell structure where the active switching element is connected to the positive power supply terminal. The conventional boost converter is inherently an N-cell boost converter.

All of these classical converters also have a mirror circuit representation. When the P-cell in a buck converter is replaced with an N-cell, the circuit takes a different configuration. In this way, the classical boost converter can be re-constructed using a P-cell, rather than an N-cell. The buck and boost converters can be easily decomposed into a P-cell and N-cell based circuit, respectively. However, this procedure is not so obvious for the buck-boost and Ćuk (boost-buck) converters; they inherently take the P-cell structure. The mirror circuit representation of each dc-dc converter is shown in the rightmost column of Fig. 3.

The construction of a P-cell circuit differs from an N-cell circuit by the relative position of the active switch. The introduction of an N-cell module simplifies the gate drive circuit because of the ground referenced gate signal. When the gate drive circuit is ground referenced, the converter circuit is more tolerant to supply noise and ripple voltage. To compare the performance of P-cell and N-cell structures, two different buck converters were simulated and tested experimentally, and the corresponding results are shown in section VI.

### V. INSIGHTS OF THE BASIC SWITCHING CELLS AND NEW DC-DC CONVERTERS

The conventional Ćuk converter has an especially unique structure [1]. A Ćuk converter has continuous input and output current, and the energy is transferred from the input to the output side by means of a capacitor. The classical Ćuk converter has an inherent P-cell structure and using the technique presented in this paper, an N-cell Ćuk converter can be achieved. A Ćuk converter is shown in Fig. 4(a), and the switching cell realization is shown in Fig. 4(b). The main limitation of the Ćuk converter is that it uses one additional inductor and capacitor. However, simplification can be done using the basic switching cells and a new version of Ćuk converter can be obtained.

In Fig. 4(a), during the time when  $S_1$  is on, the rate of change of currents in  $L_1$  and  $L_2$  is the following [14]:

$$dI_{L1}/dt = V_{in}/L_1 \quad (1)$$

$$dI_{L2}/dt = [-V_{out} - (-V_C)]/L_2 = (V_C - V_{out})/L_2 \quad (2)$$

$$\text{where } V_{out} = (t_{on}/t_{off}) \cdot V_{in} \quad (3)$$

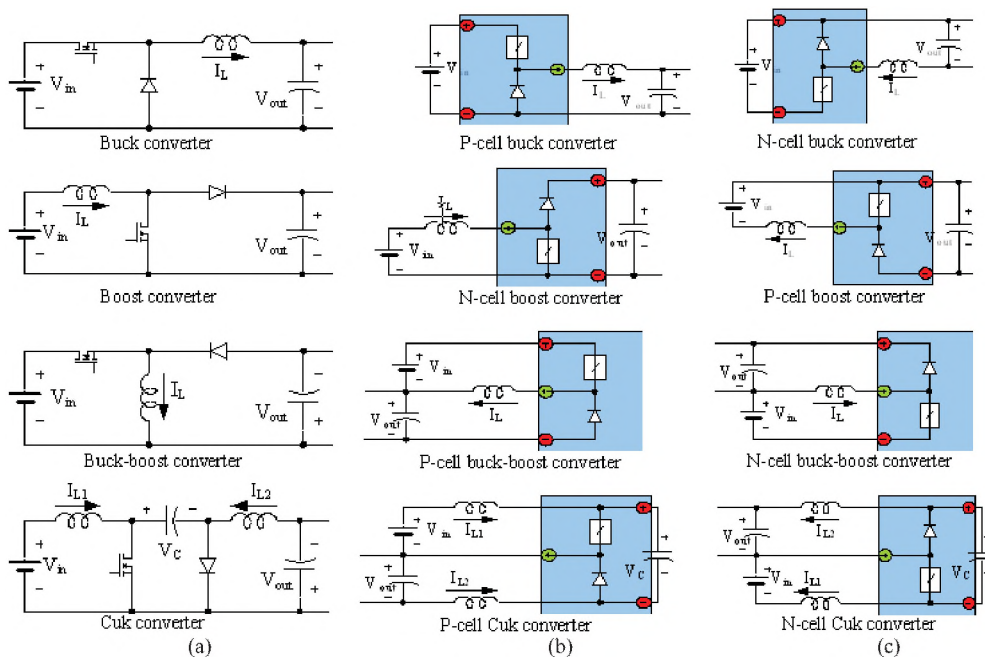


Fig. 3. (a) Classical dc-dc converters, (b) formation by the basic cells, (c) their mirror circuits.

$$\text{and } V_C = (T / t_{off}) \cdot V_{in} \quad (4)$$

Thus inserting (4) into (2),

$$dI_{L2} / dt = (1 / L_2) [(T \cdot V_{in} - t_{on} \cdot V_{in}) / t_{off}] = V_{in} / L_2 \quad (5)$$

Using the same procedure, the rate of change of currents in  $L_1$  and  $L_2$  can be found while  $S_1$  is off. When  $S_1$  is off,

$$dI_{L1} / dt = -(1 / L_1) \cdot (t_{on} / t_{off}) \cdot V_{in} \quad (6)$$

$$dI_{L2} / dt = -(1 / L_2) \cdot (t_{on} / t_{off}) \cdot V_{in} \quad (7)$$

Thus, using (1) and (5) to (7), one concludes that if  $L_1 = L_2$ , then the rate of change of currents in  $L_1$  and  $L_2$  are the same. Moreover,

$$I_{L1(avg)} / I_{L2(avg)} = I_{in} / I_{out} = D / (1 - D) \quad (8)$$

From (8), it is found that, for a specific case when the duty ratio  $D$  is 0.5, both inductors will have the same average value of current, and if  $L_1 = L_2$ , they will have the same current slope. Using these facts, the two inductors can be equivalently moved to the center rail and consolidated into one inductor as shown in Fig. 5. If the converter is not operating at  $D = 0.5$  or if  $L_1 \neq L_2$ , there will be a current mismatch between  $L_1$  and  $L_2$ , and the new Cuk converter configuration will perform slightly differently from the original Cuk converter (see Fig. 8 in section VI.B).

This new configuration of the Cuk converter will be advantageous over the conventional Cuk converter because of lesser part count. From Fig. 4(c), it is obvious that the new Cuk converter is very similar to the P-cell buck-boost converter, except for the capacitor across the positive and negative terminals of the P-cell. In practical use, it is necessary to place a decoupling capacitor in the buck-boost converter, which makes the buck-boost converter identical to the Cuk converter. Thereby, introducing the P-cell and N-cell structures it is possible to create a link between these two converters. Moreover, new converter topologies can be developed using these basic switching cells. The new Cuk converter presented in this paper is an example of many potential new circuit topologies.

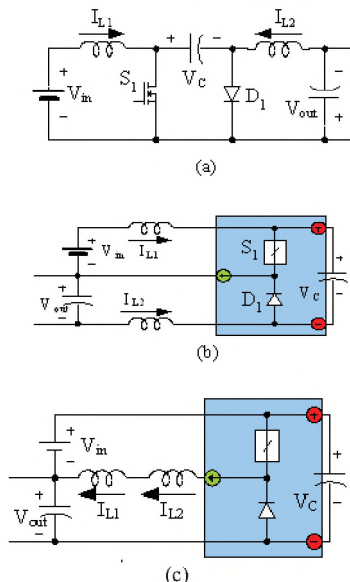


Fig. 4. a) Cuk converter, b) P-cell Cuk converter, (c) schematic of the new Cuk converter. Moving the two inductors of the Cuk converter to the center rail and combining them into one.

## VI. DC-DC CONVERTER SIMULATION AND EXPERIMENTAL RESULTS

### A. Buck Converter

To validate the concept of the P-cell and N-cell relationship, a buck converter was simulated and tested under

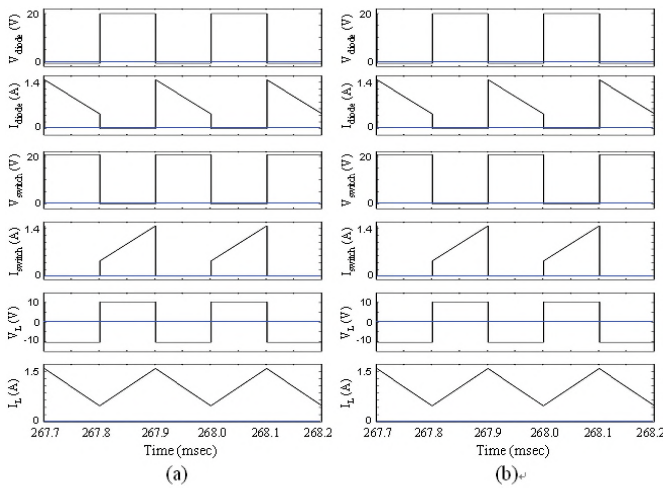


Fig. 5. Simulation results of (a) N-cell buck converter with continuous conduction, (b) P-cell buck converter with continuous conduction, (c) N-cell buck converter with discontinuous conduction, (d) P-cell buck converter with discontinuous conduction.

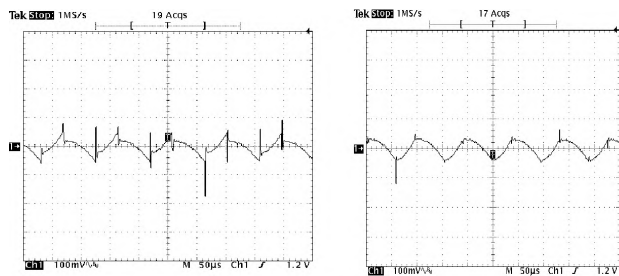


Fig. 6. Experimental output voltage ripple (100 mV/div) of buck converter, a) P-cell, b) N-cell.

continuous and discontinuous conduction mode. The simulations were done in PSIM and the results are shown in Fig. 5. However, there was no difference found in the simulation results, which leads to the conclusion that there is a mirror relationship between the N-cell and P-cell structures. Then for further verification, a pair of buck converters (one P-cell and one N-cell) were constructed from discrete components and tested in the lab in continuous conduction mode. The operating and loading conditions of the N-cell buck converter and the

P-cell circuit were the same, but some slight differences were observed in their output voltage. The test results are shown in Fig. 6.

The test setup was as follows:  $V_{in} = 20$  V,  $D = 0.4$ ,  $f_S = 10$  kHz,  $C_l = 100$   $\mu$ F,  $L_l = 1$  mH,  $D_l =$  MURB1020CT-1,  $S_l =$  IRG4BC30U,  $R_L = 20$   $\Omega$ .

For an input voltage of 20 V and duty cycle 0.4, the dc output voltage for the N-cell structure was 6.82 V and for the P-cell buck converter, it was 7.07 V. Fig. 6(a) and (b) show the output ripple components of the P-cell and N-cell structure respectively. The fundamental frequency component present in the ripple was the same for both topologies. However, the N-cell structure produces a cleaner output because of the ground-referenced gate drive circuit.

### B. Ćuk Converter

The previous section shows that the classical Ćuk converter is inherently a P-cell structure. Thereby, there exists a mirror circuit of it, which is the N-cell Ćuk converter. When the two inductors are transferred to one branch such that only one inductor is needed, one gets the third version of the Ćuk converter. To introduce the advantages of basic switching cells, three different kinds of Ćuk converters were constructed and tested. Fig. 7 shows the output voltages of these converters for a 20  $\Omega$  resistive load with a supply voltage of 20 V. The duty cycle of the gate drive was kept at approximately 0.33, and for this duty cycle, the output voltage of a Ćuk converter should be around 10 V. In Fig. 7(d)-(f), the output ac ripple is shown by zooming the dc output voltage.

Fig. 7 shows that these three converters are fairly equivalent. For the same duty cycle, the P-cell and the N-cell structures produce a 10.6 V dc output, while the new combined inductor topology produces 10.1 V dc output. These are shown in Fig. 7(a), (b) and (c) respectively. The ripple component in the N-cell circuit has the lowest amplitude of 220 mVp-p compared to the P-cell structure producing 270 mVp-p. However, the new topology with the two combined inductors produces a ripple of 340 mVp-p, which is slightly higher than the other two topologies. Fig. 7(d)-(f) show the ripple components in the three configurations.

## VII. CONSTRUCTING VOLTAGE SOURCE INVERTERS FROM THE BASIC CELLS

Like the dc-dc converters, inverters can be constructed by the use of basic cells in a similar way. Fig. 8(a) shows that the parallel combination of the P- and N- cells creates a phase leg providing bi-directional current flow. Fig. 8(b) shows the conventional anti-parallel diode/transistor configuration to create a bi-directional current flow. The parallel connection of a P-cell and an N-cell shown in Fig. 8(a) has some distinct advantages over the conventional IGBT with an anti-parallel diode.

To create a bi-directional current port in a VSI, two transistors in a phase leg are switched periodically. However, there is a requirement of dead time between the switching periods of the two transistors that prevents a short circuit of the dc link. When

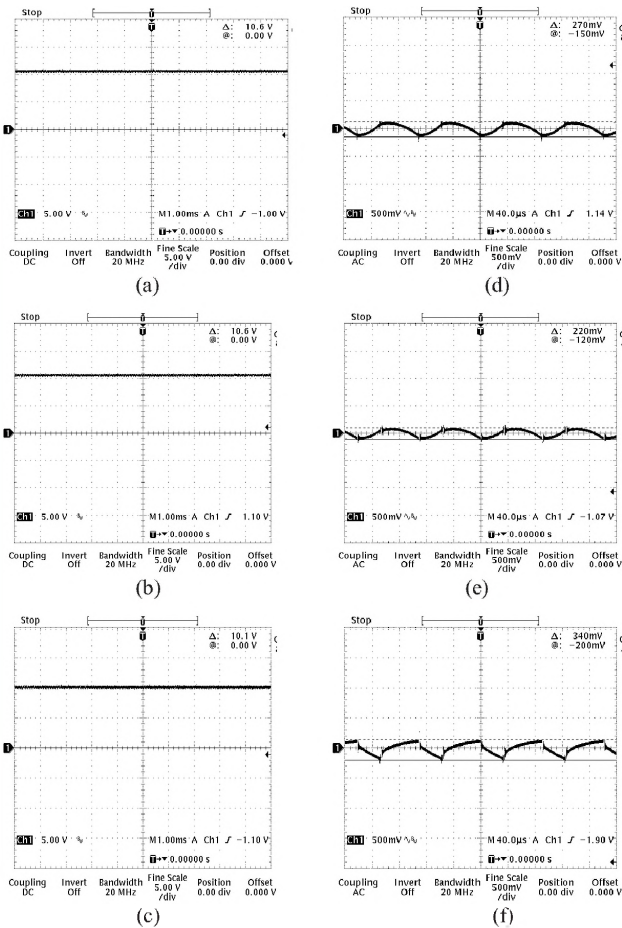


Fig. 7. Experimental output voltage of the converters . (a) P-cell Ćuk converter dc output voltage (5V/div). (b) N-cell Ćuk converter dc output voltage (5V/div). (c) new Ćuk converter dc output voltage (5V/div). (d) output ripple of P-cell Ćuk converter (500mV/div). (e) output ripple of N-cell Ćuk converter (500mV/div). (f) output ripple of new Ćuk converter (500mV/div).

an inductor is placed in the paralleled P-cell and N-cell configuration, it takes the shape of Fig. 8(c). In this case, a dead time is not required because the additional inductor and the stray inductance of the interconnections limit the current if there is any overlap in the switching of the P-cell and N-cell devices. Therefore, IGBT-diode modules configured as the P- and N-cell are better suited for inverter operation, and at any instant of time, the load current only goes through the P-cell during the positive half cycle and through the N-cell during the negative half cycle of the current. Moreover, for a modulation scheme that can detect the direction of current to the load, only the switch that provides the current path needs to be switched while the other can be kept off. In the VSI circuit shown in Fig. 8(b), when the current is going to the load, the transistor in the P-cell is switched on and the transistor in the N-cell is kept off. In the same way, when the current is coming back from the load, it flows through the transistor in the N-cell which is switched on, and the transistor in the P-cell is kept off.

Fig. 9 shows the series connection of the P- and N- cells, which forms a three-level (flying capacitor) converter and

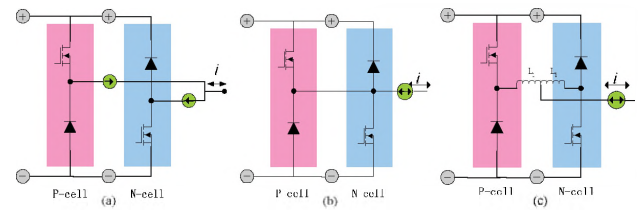


Fig. 8. a) An inverter phase leg with bidirectional current flow by paralleling the P- and N-cells, b) conventional connection of anti-parallel diode, c) placing two inductors between P-cell and N-cell common terminals to limit current change rate.

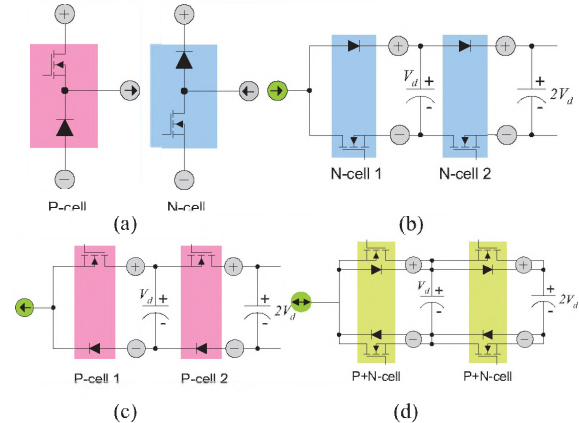


Fig. 9. A three-level (flying capacitor) converter is formed by the series connection of the P- and N-cells, a) a P and N-cell, b) series connection of two N-cells, c) series connection of two P-cells, d) parallel connection of (b) and (c).

inverter [15]. Similarly, the diode clamped multilevel inverter and the generalized multilevel inverter structure [16] can be constructed in this manner. In Fig. 9, the series connection uses the same voltage polarity, thus adding voltage to a higher level. Again, it is obvious from these circuits that IGBT-diode modules should be assembled and built according to the P- and N-cell structures.

When two basic switching cells are connected in series to generate a flying capacitor voltage, a new kind of switching cell is obtained. In Fig. 9(a), when two N-cells are connected in series, N-cell 2 becomes a new 4-terminal switching cell, which is different from N-cell 1. In the same way, P-cell 2 is different from P-cell 1. This phenomenon was also observed in Fig. 10 (a) and (b) while two switching cells were connected in series to generate an ac port. In addition to that, all the terminologies for P-cell and N-cell used in creating an ac port in Fig. 10 were valid while  $v_{ac}$  was smaller than  $V_d$ .

## VIII. CURRENT SOURCE INVERTER FROM BASIC SWITCHING CELLS

A current source inverter (CSI) has several key applications in industry. Fig. 11(b) shows a conventional CSI where the load is a series connection of a resistor and an inductor. Four switches  $S_1$ ,  $S_2$ ,  $S_3$ , and  $S_4$  are operated in pairs so that an alternating current can flow through the load. To get the alternating current,  $S_1$  and  $S_4$  are operated during the positive half cycle of the

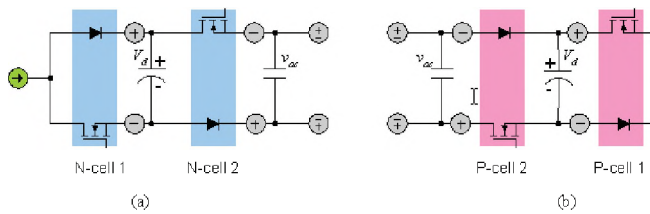


Fig. 10. Series connection of the N-cells and P-cells to form an ac voltage port. a) an ac voltage port is created from a current source. b) a current source is created from an ac voltage port.

current, whereas,  $S_2$  and  $S_3$  are switched on during the negative half cycle or vice-versa.

To form a VSI, a P-cell and an N-cell are connected in parallel to build a block, and two blocks in parallel form the entire VSI. However, the mirror structure of this VSI construction is followed to build the series combination of a P-cell and an N-cell, and thus a new type of CSI can be formed. This is shown in Fig. 10(a), where two N-cells form an ac voltage port from a current source. Fig. 10(b) shows the series combination of two P-cells to obtain a current source from an ac voltage input.

If the two blocks depicted in Fig. 11 are connected together, a new single-phase current-source inverter can be constructed as shown in Fig. 11(a). By eliminating the two middle capacitors ( $C_1$  and  $C_2$ ) in this inverter, the traditional current-source inverter can be obtained as shown in Fig. 11(b). The traditional current-source inverter experiences difficulties with voltage over-shoot at turn-off and a current commutation problem that requires over-lap time from one phase leg to another. However, the new current-source inverter in Fig. 11(a) has no voltage overshoot and no current commutation problem.

The capacitor  $C_1$  ( $C_2$ ) with the two diodes form a lossless snubber providing voltage clamping to the switching devices and a current path to the current source, thus improving reliability.

To demonstrate some of the advantage of the new topology, a current source inverter was synthesized using the basic switching cells. The new circuit has no voltage overshoot as compared to the traditional CSI (illustrated in Fig. 12(a)) and has less output power ripple (shown in Fig. 12(b)). A constant load of 1 kW was used for the simulation of both converter types. The new topology can be implemented in several different inverter types. Multilevel inverters with voltage balancing features can be constructed using these basic switching cells, and thus it becomes easier to analyze the entire circuit. In Fig. 12(a), the  $V_{DS}$  across  $S_1$  and  $S_4$  is shown and the new converter shows better performance than the conventional converter. In Fig. 12(b), the input and output power of the two converters are compared. The input power of the conventional converter has more ripple than that of the new converter. Moreover, the switches in the new converter experience less voltage ripple compared to the voltage drop across the switches in a conventional converter. An R-L load ( $10 \Omega + 100 \mu\text{H}$ ) was used for the simulation. Two  $1 \mu\text{F}$  electrolytic capacitors in parallel were used as the load capacitance ( $C_{out1}$  and  $C_{out2}$ ). The

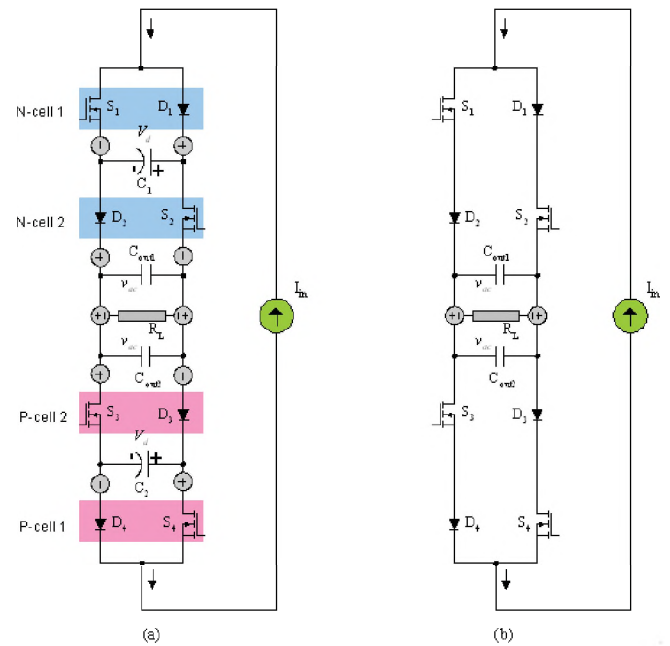


Fig. 11. a) Current-source inverter with lossless snubber built from P-cell and N-cell. b) traditional current-source inverter.

experimental prototype for the P-cell and N-cell is shown in Fig. 13.

A CSI circuit was built and tested using the schematics shown in Fig. 11. Ultra fast IGBTs (IRG4BC30U) were used as the active switches in the circuit and MURB1020CT-1 diodes were used in each switching cell.

A 20 V source and a series connected 1 mH inductor were used to get a constant current source. Two  $0.01 \mu\text{F}$  polyester capacitors were used as  $C_1$  and  $C_2$ , and a  $0.1 \mu\text{F}$  polyester capacitor was used as the load capacitance. A resistor of  $20 \Omega$  was used as the output load, and the circuit was operated at 60 Hz.

Fig. 14(a) shows the  $V_{DS}$  of  $S_1$  of the new CSI and (b) shows the  $V_{DS}$  of  $S_1$  in the conventional circuit. It is clear that  $C_1$  performs the snubber operation so that the voltage across  $S_1$  cannot increase beyond the supply voltage, and without  $C_1$ , the voltage stress across  $S_1$  increases substantially in the conventional CSI. However, a small price has to be paid for this clamping feature. When  $C_1$  is used to control the  $V_{DS}$  of  $S_1$ , the  $V_{DS}$  of  $S_2$  increases slightly in the new CSI circuit. This effect of  $C_1$  on  $S_2$  is shown in Fig. 15(c) and (d). In addition to the improvement in  $S_1$ ,  $V_{DS}$  of  $S_3$  is much smaller in the new CSI circuit as well. However,  $C_1$  and  $C_2$  do not have any significant impact on the  $V_{DS}$  of  $S_4$ . It is prominent that the total improvement in the  $V_{DS}$  of  $S_1$  and  $S_3$  is much greater than the increased voltage stress across  $S_2$ .

For the same operating condition, no significant difference was found between the output voltages for the new and conventional CSI circuit. It was true for the input current too. Moreover, the ripple present in the input current is slightly less in the new CSI circuit compared to the conventional CSI circuit.

## IX. CONCLUSIONS

The basic switching cells presented in this paper are not limited to the applications described in this paper. The advantages of using P-cells and N-cells in dc-dc converters and current source inverters have been described with simulation and experimental results. From the experimental results, it was found that N-cell dc-dc converter circuits have smaller ripple at the output for the same operating condition. The new CSI circuit constructed from basic switching cells experiences much smaller voltage stress across the transistors and thereby, it increases the reliability of the circuit. However, the most advantageous part of the switching cell concept is that it creates a new vision to analyze the conventional power electronic converters by segregating them into smaller modular blocks. This modeling approach is not limited to the use basic switching cells for analysis of existing power electronic circuits. Rather, it is a means to find different modular patterns in power electronic circuits, which can lead to several new circuit topologies.

## REFERENCES

- [1] S. Čuk, "General Topological Properties of Switching Structures," *IEEE Power Electronics Specialists Conference Record*, 1979, pp. 109-130.
- [2] R. D. Middlebrook, S. Čuk, "A General Unified Approach to Modeling Switching-Converter Power Stages," *IEEE Power Electronics Specialists Conference*, 1976, pp. 18-34.
- [3] S. Čuk, R. D. Middlebrook, "A General Unified Approach to Modeling Switching DC-to-DC Converters in Discontinuous Conduction Mode," *IEEE Power Electronics Specialists Conference*, 1977, pp. 36-57.
- [4] A. Pietkiewicz, D. Tollik, "Unified Topological Modeling Method of Switching DC-DC Converters in Duty-Ratio Programmed Mode," *IEEE Trans. Power Electronics*, vol. 2, no. 3, 1987, pp. 218-226.
- [5] T.-F. Wu, Y.-K. Chen, "Modeling PWM DC/DC Converters out of Basic Converter Units," *IEEE Trans. Power Electronics*, vol. 13, no. 5, Sept. 1998, pp. 870-881.
- [6] J. Chen, K. D. T. Ngo, "Alternate Forms of the PWM Switch Model in Discontinuous Conduction Mode," *IEEE Trans. Aerospace and Electronic Systems*, vol. 37, no. 2, April 2001, pp. 754-758.
- [7] E. E. Landsman, "A Unifying Derivation of Switching DC-DC Converter Topologies," *IEEE Power Electronics Specialists Conference (PESC'79)*, June 18-22, 1979, San Diego, pp. 239-243.
- [8] R. Erickson, D. Maksimovic, *Fundamentals of Power Electronics*, 2nd edition, Kluwer Academic Publishers, 2001.
- [9] F. Z. Peng, L. M. Tolbert, F. H. Khan, "Power Electronic Circuit Topology – the Basic Switching Cells," *IEEE Power Electronics Education Workshop*, June 16-17, 2005, Recife, Brazil.
- [10] Y. Guo, M. M. Morcos, M. S. P. Lucas, "On the Canonical Switching Cell for DC-DC Converters," *North American Power Symposium Proceedings*, Oct. 11-12, 1993, Washington, DC, pp. 672-681.
- [11] John G. Kassakian, Martin F. Schlecht, and George C. Verghese, *Principles of Power Electronics*, Addison Wesley Publishing Company, 1991, Chapter 6.
- [12] T.-F. Wu and Y.-K. Chen, "Modeling PWM DC/DC Converters out of Basic Converter Units," *IEEE Trans. on Power Electronics*, vol. 13, no. 5, pp. 870-881, Sep. 1998.
- [13] Tsai-Fu and Yu-Kai Chen, "A Systematic and Unified Approach to Modeling PWM DC/DC Converters Based on the Graft Scheme," *IEEE Trans. on Industrial Electronics*, vol. 45, no. 1, pp. 88-98, Feb. 1998.
- [14] A. I. Pressman, *Switching Power Supply Design*, New York: McGraw-Hill, 1998, Chapter 6.
- [15] T. A. Meynard, H. Foch, "Multilevel Conversion: High Voltage Choppers and Voltage Source Inverters," *IEEE Power Electronics Specialists Conference (PESC'92)*, vol. 1, pp. 397-403, June 29-July 3, 1992.
- [16] F. Z. Peng, "A Generalized Multilevel Inverter Topology with Self Voltage Balancing," *IEEE Trans. on Industry Applications*, vol. 37, no. 2, March/April 2001, pp. 611-618.

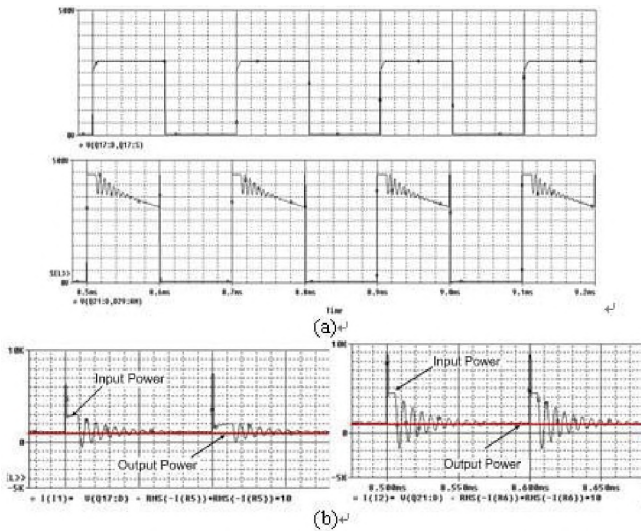


Fig. 12. a) Comparison of drain to source voltage of the switches in the current source inverter. The top figure shows the  $V_{DS}$  for the new converter and the bottom figure shows the  $V_{DS}$  for the conventional converter. b) Input and output power wave shapes of the two converters. The output power is a constant line at a level of 1 kW. (Left is the new one, right is the conventional one).



Fig. 13. The experimental prototype of the P-cell and N-cell. The upper left section shows the P-cell, the upper right section shows an N-cell. The bottom part of the board shows the gate drive circuit.

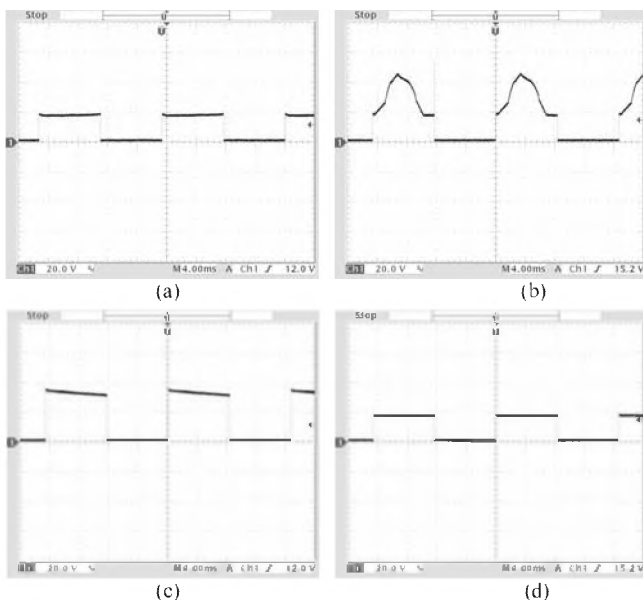


Fig. 14. Experimental voltage waveforms for a conventional and new CSI circuit. (a)  $V_{DS}$  of  $S_1$  in the new CSI circuit, (b)  $V_{DS}$  of  $S_1$  in the conventional CSI circuit, (c)  $V_{DS}$  of  $S_2$  in the new CSI circuit, (d)  $V_{DS}$  of  $S_2$  in the conventional CSI circuit (all voltages are scaled at 20 V/div).